ACS Partner Journal

CHEM & BIO ENGINEERING

pubs.acs.org/ChemBioEng

Article

Rational Design of Superhydrophobic and Flexible Oriented MOF Nanosheet Membrane for Highly Efficient Ethanol–Water Separation

Wei Shao, Xiao-Feng Zhong, Yi-Le Chen, Zhen Chen, Miao-Miao Jia, Wen-Yong Yang, Jing-Ran Yu, Pan-Pan Zhang, Yi Li,* and Ming Xue*

Cite This: *Chem Bio Eng.* 2025, 2, 332–340

Read Online

ACCESS | Metrics & More | Article Recommendations | Supporting Information

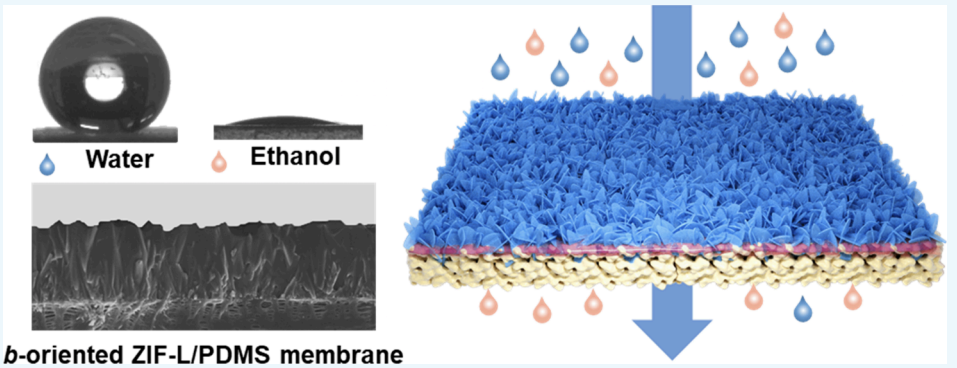

ABSTRACT: Highly efficient and energy-conserving membrane separation technology holds vast potential for applications in the bioethanol production process. This work reports a strategy for the fast preparation of an oriented and flexible two-dimensional metal–organic framework (MOF) nanosheet membrane by an electrochemical deposition method. The oriented MOF nanosheet membrane growth, followed by spin-coating of polydimethylsiloxane, resulted in an efficiently formed superhydrophobic and ethanol affinity membrane for separating ethanol from aqueous solution. Vertically aligned MOF nanosheets with strong ethanol affinity and superhydrophobic membrane surfaces simultaneously promote the transport process, thus delivering a relatively high flux of 1.63 kg·m^{-2}·h^{-1} and good separation factor of 14.89 in the pervaporation of 5 wt % ethanol aqueous solution. The oriented arrangement of MOF nanosheets combined with polydimethylsiloxane can significantly enhance the pervaporation selectivity and flux, creating a preferential pathway for the production of biofuel.

KEYWORDS: *Metal–organic framework, Membrane, Electrochemical deposition, Superhydrophobic, Pervaporation*

1. INTRODUCTION

Bioethanol is a renewable energy source with extensive application prospects and important environmental benefits.[1,2] It is primarily produced through a fermentation process and then purified. During the biological fermentation process, the increase in ethanol concentration can inhibit microbial activity and limit fermentation efficiency. Therefore, the timely removal of ethanol from the fermentation broth is crucial to ensure the continuous progress of fermentation and to enhance ethanol production. To address the aforementioned issue, purification technologies of distillation, membrane separation, ionic liquid extraction, and biosorption were developed.[3−7] Pervaporation derived from membrane separation with high efficiency and low energy penalty has emerged as a new promising method for the production of high-purity ethanol. The pervaporation separation performance is critically associated with the efficiency of membrane materials.[8,9] Polymer membranes are widely used for pervaporation due to their low cost and good flexibility.[10] However, polymer membranes frequently encounter a balance issue between the permeability and selectivity. Therefore, developing and fabricating high-performance membranes that can maintain both high permeability and high selectivity in practical ethanol–water separation applications remain significant challenge.

Metal–organic frameworks (MOFs) are highly promising for membrane separation due to their ultrahigh specific surface area, adjustable pore structures, customizable chemical properties, and exceptional adsorption capabilities. MOF membranes often

Received: January 13, 2025
Revised: March 12, 2025
Accepted: March 17, 2025
Published: March 28, 2025

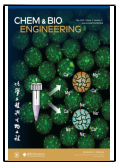

show higher selectivity and permeability as well as excellent durability.[11−18] Controlling the microstructure, grain orientation, intergranular defects, and thickness of MOF membranes is crucial for enhancing separation performance.[19−24] It is worth noting that compared to nonoriented MOF membranes, the oriented intergrowth of the MOF membrane could significantly minimize the intergranular defects, avoiding filler aggregation and improving separation selectivity, which could further reduce molecular diffusion resistance and increase permeability. For example, the oriented ZIF-95 membrane prepared by vapor-assisted in-plane epitaxial growth exhibited good hydrogen permeance that was 4.6 times higher than that of nonoriented membranes, which was attributed to the excellent oriented structure with less grain defects and transport pathways.[25] Uniform triangular UiO-66 nanoplate seeds were prepared by an anisotropic etching process, and subsequently, highly oriented ultrathin UiO-66 membranes with counter-diffusion growth were obtained. These membranes exhibit unprecedented CO_2 permeance and excellent CO_2/N_2 selectivity, and the precise etching process seed provides an effective guarantee for the growth of highly oriented membranes.[26] A flexible and reversible deformation MOF nanosheet membrane underwent controlled growth on a polymer substrate; oriented growth of nanosheets offers rapid molecular channels, leading to ultrahigh flux during alcohol−water permeation separation.[27] However, the majority of previous membranes usually require the synthesis of crystal seeds, subsequently preparing them as oriented membranes. This process usually requires a high degree of uniformity in the dispersion of crystal seeds, and the procedure demands precise manipulation skills. It should be noted that merely controlling the orientation of the membrane is not sufficient; the polycrystalline membrane still needs to undergo a series of mechanical performance tests in practical applications. Combining an oriented polycrystalline membrane with a flexible polymer can significantly enhance the mechanical properties. This combination not only improves the strength and toughness of the membranes but also enhances their durability and adaptability in practical applications. Recently, $Zn_2(bim)_4$ was vertically grown on a PVDF substrate and combined with an ultrathin polyamide film. This composite membrane induced an extremely high H_2/CO_2 selectivity of 1084. Furthermore, the membrane maintained stable separation performance after undergoing 50-fold reversal at 90°.[28] A spin-coating method was used to assemble MOF particles on a poly(vinylidene fluoride) substrate and form an oriented monolayer membrane, utilizing a polymer to seal the gaps between the particles. The pervaporation separation performance for aromatic−aliphatic hydrocarbon mixtures is 3 to 10 times higher than that of traditional randomly oriented mixed matrix membranes, and exhibits good flexibility and antiswelling properties.[29] On this basis, our method aims to electrochemically rapidly prepare an oriented MOF membrane that effectively combines with polymers to enhance synergistic effects, thereby constructing quickly oriented separation channels and good mechanical properties to improve separation efficiency.

In this work, a superhydrophobic *b*-oriented ZIF-L/PDMS composite membrane was quickly synthesized on a polymer substrate at ambient temperature in aqueous solution. A constant current was employed to facilitate the rapid migration of metals and ligands for the self-assembly of *b*-oriented ZIF-L membranes, and then an ultrathin PDMS protective layer was spin-coated to form a superhydrophobic ZIF-L/PDMS composite membrane. The *b*-oriented ZIF-L membrane can supply the rapid penetration channels of ethanol, while the hydrophobic PDMS further enhances the ethanol affinity and hydrophobicity of the ZIF-L membrane, thereby enhancing the selectivity of separating ethanol from aqueous solution. Therefore, the well-synthesized ZIF-L/PDMS composite membrane is expected to exhibit excellent separation performance with a relatively high flux of 1.64 $kg·m^{-2}·h^{-1}$ and good separation factor of 15.6 in the pervaporation of 5 wt % ethanol aqueous solution. In addition, this superhydrophobic ZIF-L/PDMS composite membrane exhibits good flexibility and stability, which can be adapted to practical separation applications for biofuel production.

2. EXPERIMENTAL SECTION

2.1. Experiment Materials. Zinc nitrate hexahydrate ($Zn(NO_3)_2·6H_2O$, >99.99%) was purchased from Xilong Science Co., Ltd., 2-Methylimidazole (2-MeIm, >99%) was purchased from Adamas, *n*-heptane (analytical reagent) was purchased from Shanghai Maclin Biochemical Technology Co., LTD, and PDMS (polydimethylsiloxane, Dow Corning Sylgard184) was purchased from Guangzhou Lige Technology Co., Ltd. All chemicals were used without further purification. The polypropylene support membrane's diameter is 25 mm and average pore size is between 200 and 500 nm.

2.2. Preparation of ZIF-L Membrane. The synthesis solution of the ZIF-L membrane was prepared by using 3.28 g (40 mmol) of 2-MeIm to dissolve in 50 mL of H_2O, while 1.48 g (5 mmol) of $Zn(NO_3)_2·6H_2O$ was dissolved in another 50 mL of H_2O. The two solutions were stirred until all solids were completely dissolved. Then the metal salt solution was slowly added into the 2-MeIm solution for the electrochemical synthesis of the ZIF-L membrane. The Au−Pd coated PP (Polypropylene) substrate was used as the working electrode, and a foil electrode was applied as the counter electrode, both of which were parallelly immersed into the ZIF-L synthesis solution with a distance of 3 cm. For the in situ electrochemical synthesis, a constant current of 0.02 mA/cm^2 was applied to get the *b*-oriented ZIF-L membrane at room temperature for 45 min. Finally, the *b*-oriented ZIF-L membrane was washed with water three times and dried at room temperature. PDMS modified the surface of the *b*-oriented ZIF-L membrane: the homogeneous PDMS solution was prepared by adding 0.5−2 g (9−28.5 wt %) of Dow Corning PDMS polymer and 0.05−0.2 g of cross-linking agent into 5 g of *n*-heptane. The mixing solution was stirred for 1 h, and then 50−200 μL of PDMS was spin-coated on the surface of the *b*-oriented ZIF-L membrane at speeds of 1500 rpm for 30 s and 3000 rpm for another 30 s. Afterward, the membranes were kept in a vacuum oven at 80 °C for 12 h. The membrane was named as ZIF-L/PDMS-*X* composite membrane, where *X* represents the spin-coating amount of PDMS. This work focuses on the ZIF-L/PDMS-100 composite membrane prepared by spin-coating 100 μL of 16.6 wt % PDMS as the main research subject to explore its pervaporation separation performance.

2.3. Characterization. The phase structure of the ZIF-L membrane was characterized by Powder X-ray diffraction (XRD, Ultima IV Rigaku) with Cu Kα radiation. The ATR-IR patterns of the ZIF-L membrane were characterized by using a Thermo Scientific Nicolet iS50 instrument. XPS measurement was taken by using a Shimadzu AXIS SUPRA$^+$ instrument. The microstructure of the ZIF-L membrane was observed by scanning electron microscopy (SEM; Thermo Fisher Axia) and atomic force microscopy (AFM; Bruker Dimension Icon). Water

https://doi.org/10.1021/cbe.5c00006
Chem Bio Eng. 2025, 2, 332−340

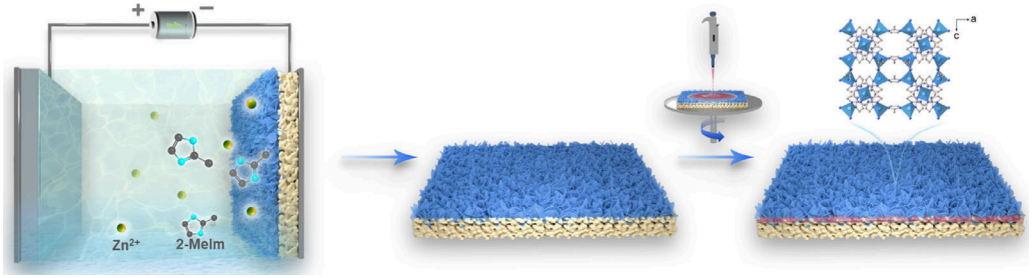

Figure 1. Illustration of preparing the superhydrophobic *b*-oriented ZIF-L/PDMS composite membrane.

contact angles were tested by using a German Dataphysics OCA20 instrument. The adsorption capabilities of the ZIF-L powder for water and ethanol were evaluated with a vapor sorption analyzer (BSD-VVS, China).

2.4. Gas Separation Test of ZIF-L/PDMS-100 Membrane. The separation performance test was assessed using the Wicke-Kallenbach method; the total flow rate of mixed H_2/CO_2 volume was maintained at 100 mL/min (each gas was 50 mL/min), and Ar was employed as the sweep gas at a flow rate of 25 mL/min.

2.5. Ethanol−Water Separation Performance of ZIF-L/PDMS Membranes. The ethanol−water separation performance of these membranes was tested by using a homemade permeation cell, and the pervaporation test diagram is shown in Figure S1. The ethanol percent in the feed solution was 5 wt %, and the feed temperature ranged from 30 to 60 °C. Gas chromatography (Agilent 8890) was used to analyze the permeation component. The separation performance of permeation total flux (J) and separation factor ($\alpha_{EtOH/water}$) was calculated by eqs 1 and 2 as follows:

$$J = \frac{W}{A \times t} \tag{1}$$

$$\alpha_{EtOH/water} = \frac{Y_{p-EtOH}/Y_{p-water}}{X_{f-EtOH}/X_{f-water}} \tag{2}$$

where W is the total permeation weight, t is the collected hours, A is the efficient area of membrane. Y_{p-EtOH} and $Y_{p-water}$ are the weight fraction of ethanol and water in the permeate, X_{f-EtOH} and $X_{f-water}$ are the weight fraction of ethanol and water in the feed.

3. RESULTS AND DISCUSSION

3.1. Characterization of ZIF-L Membranes. In this work, an electrochemical fast synthesis strategy was employed to fabricate a oriented ZIF-L membrane on a flexible PP substrate at ambient temperature in aqueous solution, and then an ultrathin PDMS layer was spin-coated on a ZIF-L membrane to obtain the ZIF-L/PDMS composite membrane (Figure 1). The XRD analysis of ZIF-L nanosheets aligns closely with simulation data, indicating the high purity and crystallinity of ZIF-L (Figure S2a). Additionally, SEM imaging reveals that the ZIF-L nanosheets exhibit a distinctive leaf-shaped nanosheet morphology (Figure S2b). More importantly, ZIF-L nanosheets exhibit a significant difference in affinity between ethanol and water, and the water contact angle photograph shows that ZIF-L nanosheets are hydrophobic, while the contact angle for ethanol is only 13° (Figure S2c,d). These results are sufficient to demonstrate that ZIF-L nanosheets are an excellent membrane material for separating ethanol from aqueous solution.

The precursor solution is of paramount importance for the electrochemical synthesis, as it significantly influences the crystal nucleation and orientated growth. The XRD patterns revealed the well-defined crystallinities of the ZIF-L membrane with 0.05 M Zn^{2+}, confirming the successful electrochemical synthesis. Furthermore, the characteristic peaks of the membrane at 10.36° correspond to the (020) planes of the ZIF-L, clearly demonstrating that the membrane manifested a highly *b*-out-of-plane oriented arrangement (Figure S3a). According to the Van der Drift growth model, the growth rate of the crystal is faster along the *b* direction. Compared to the synthesis without an electric field (Figure S4), the guidance of an electric field further accelerates the growth rate in a high concentration precursor solution, resulting in a more pronounced orientation of the crystal in the *b* orientation, thereby forming a dense *b*-oriented ZIF-L membrane. Moreover, there is no obvious difference between *b*-oriented ZIF-L and *b*-oriented ZIF-L/PDMS membranes, indicating that the spin-coated PDMS does not affect the membrane orientation and crystal structure. To gain more evidence of PDMS, FTIR-ATR spectroscopy was applied. The ZIF-L membrane displays the characteristic bond peaks at 1568 and 1307 cm^{-1} for the C−N and C═N stretching vibrations on the imidazole ring from ZIF-L. Another two peaks at 1145 and 755 cm^{-1} are attributed to the bending vibrations of C−H and C−N. By comparison, the ZIF-L/PDMS composite membrane shows three new peaks at 1086, 1012, and 1259 cm^{-1}, which can be ascribed to the stretching vibration of Si−O−Si, symmetric bending, and stretching vibration of CH_3 in Si-CH_3, respectively (Figure S3b). These results strongly confirm the successful modification of PDMS on the ZIF-L membrane. XPS spectroscopy shows that the Zn 2p peak intensity of ZIF-L membrane decreases, and the binding energy is slightly shifted after spin-coating of PDMS due to the unsaturated Zn in the ZIF-L nanosheet forming a new coordination bond with the O atoms from PDMS (Figure S3c). Additionally, the Si−O peak was fitted into two peaks of Si−O−Si (102.5 eV) and Si−O−Zn (101.8 eV) with the existence of PDMS on the membrane surface (Figure S 3d).

Compared with the well intergrown ZIF-L membrane, the top view of the ZIF-L/PDMS-100 composite membrane shows there are no visible defects, pinholes, or cracks on the membrane surface (Figure 2a, b). Cross-sectional SEM images showed the good orientation and denser structure of the ZIF-L membrane, and the thickness is about 5 μm (Figure 2c). EDS mapping shows the zinc and silicon elements are uniformly distributed (Figure 2d). In addition, PDMS is a hydrophobic material with good fluidity, it helps to further increase the ethanol affinity of ZIF-L membrane. In order to understand the effect of PDMS on the ZIF-L/PDMS composite membrane, different concentrations and amounts of spin-coated PDMS were investigated. When the PDMS (0.5 g) concentration is low (9 wt %), low-

https://doi.org/10.1021/cbe.5c00006
Chem Bio Eng. 2025, 2, 332−340

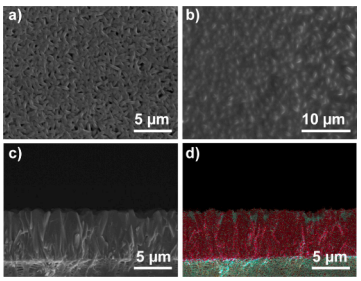

Figure 2. SEM images of (a) ZIF-L membrane, (b) ZIF-L/PDMS-100 composite membrane, and (c,d) cross-sectional view and EDS mapping of ZIF-L/PDMS-100 membrane. Si signal: green, Zn signal: red.

viscosity PDMS cannot sufficiently fill the gaps between ZIF-L nanosheet layers. Conversely, when the PDMS (2 g) concentration is high (28.5 wt %), the decreased fluidity leads to increased accumulation of PDMS on top of the ZIF-L nanosheet layers, thereby obscuring the characteristic structure of the nanosheets (Figure S5). Thus, 16.6 wt % PDMS (1 g) was chosen as the ideal preparation concentration. The amount of PDMS spin-coated is another important factor affecting the surface hydrophobicity of the membrane. PDMS cannot fully penetrate along the ZIF-L nanosheets with spin-coating of 50 μL, and there are nearly no changes in the thickness of the ZIF-L/PDMS-50 membrane (Figure S6a, b). When the spin-coated amount of PDMS increased to 100 μL, PDMS fully penetrated along the ZIF-L nanosheets, but the ZIF-L nanosheet crystals were not completely covered (Figure 2b, c). However, excess spin-coated PDMS completely covered the ZIF-L nanosheets and PDMS also appeared on the cross section that ZIF-L crystals became blurred and reduced the structural effect of ZIF-L nanosheets during the pervaporation process for separating ethanol from aqueous solution (Figure S6c-f).

To further investigate the surface properties of the ZIF-L/PDMS composite membranes, AFM was used to analyze the surface roughness of different ZIF-L/PDMS membranes. The original PP substrate showed a smooth surface, and roughness was only 38.4 nm; this indicates that the PP substrate has a relatively low roughness surface before any modification. When ZIF-L crystals grew on the PP substrate, the surface roughness of the membrane significantly increased to 108 nm (Figure S7). This is because the ZIF-L crystals possess regular shapes and nanoscale dimensions, and their deposition on the substrate surface greatly promotes the formation of surface roughness. After spin-coating PDMS, the surface roughness underwent further changes. The roughness of ZIF-L/PDMS composite membranes changed with different amounts of spin-coated PDMS (Figure 3). It can be observed that roughness tends to increase and then decrease as the amount of spin-coated PDMS increases. The maximum roughness Ra value of the ZIF-L/PDMS membrane is 169 nm, while the minimum roughness Ra value of the ZIF-L/PDMS membrane is only 57.4 nm. These results can be interpreted as follows: an appropriate amount of spin-coated PDMS can help fill the grain boundary of the ZIF-L without completely covering the ZIF-L nanosheet crystals and keep a high proportion of ZIF-L, which is beneficial to maintain a rough surface and improve roughness, thereby facilitating the formation of a superhydrophobic and ethanol affinity surface on the composite membrane. On the contrary, an excess amount of spin-coated PDMS would completely cover the ZIF-L crystal, leaving a smoother PDMS layer and less surface wrinkles, resulting in decreasing roughness, and the separation function of the ZIF-L crystal layer was also difficult to utilize.

The ZIF-L/PDMS composite membrane exhibits superhydrophobicity and ethanol affinity performance, which is due to the effective combination of micronanostructures formed by the oriented ZIF-L layer and superhydrophobic PDMS. The water contact angle of the original PP substrate is 98° (Figure S8), while that of the ZIF-L/PP membrane increased to 126° after ZIF-L nanosheet growth; this indicated an increase in the hydrophobicity of the membrane. Remarkably, the water contact angle of the ZIF-L membrane showed a trend of increasing first and then decreasing as the amount of spin-coated PDMS increased. When the amount of spin-coated PDMS increased to 100 μL, the water and ethanol contact angles of ZIF-L/PDMS composite membrane reached 155° and 11°, respectively. The rolling angle test result indicates that water droplets begin to roll off the ZIF-L/PDMS-100 membrane surface at an extremely low tilt angle of 9° (Video S1). These results demonstrate the formation of superhydrophobic and ethanol affinity surfaces (Figure 4a). This is due to a small amount of PDMS not completely covering the ZIF-L nanosheets; a high proportion of ZIF-L nanosheets can help form high roughness and micronanostructures. Then the affinity for ethanol is increased and hinders the penetration of water. In addition, there is a significant difference in the adsorption of water and ethanol by ZIF-L nanosheets. The adsorption

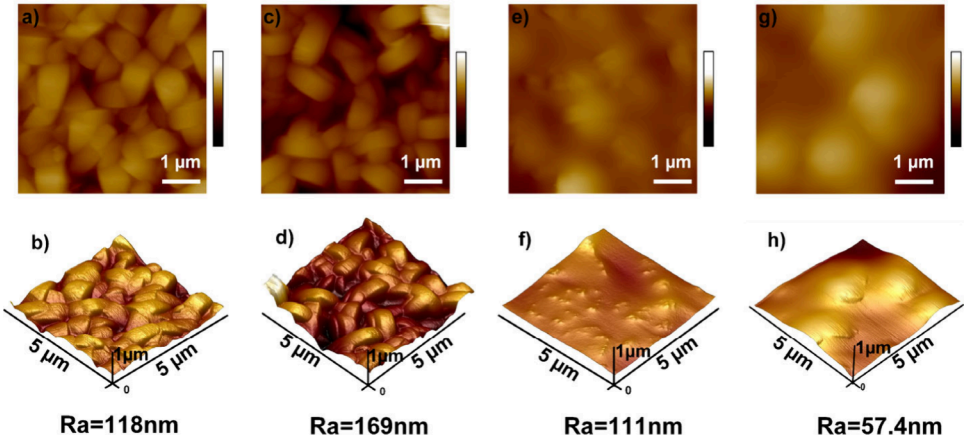

Figure 3. 2D AFM and 3D surface structure images of ZIF-L membrane spin-coated with different amounts of PDMS: (a, b) 50 μL, (c, d) 100 μL, (e, f) 150 μL, and (g, h) 200 μL.

https://doi.org/10.1021/cbe.5c00006
Chem Bio Eng. 2025, 2, 332−340

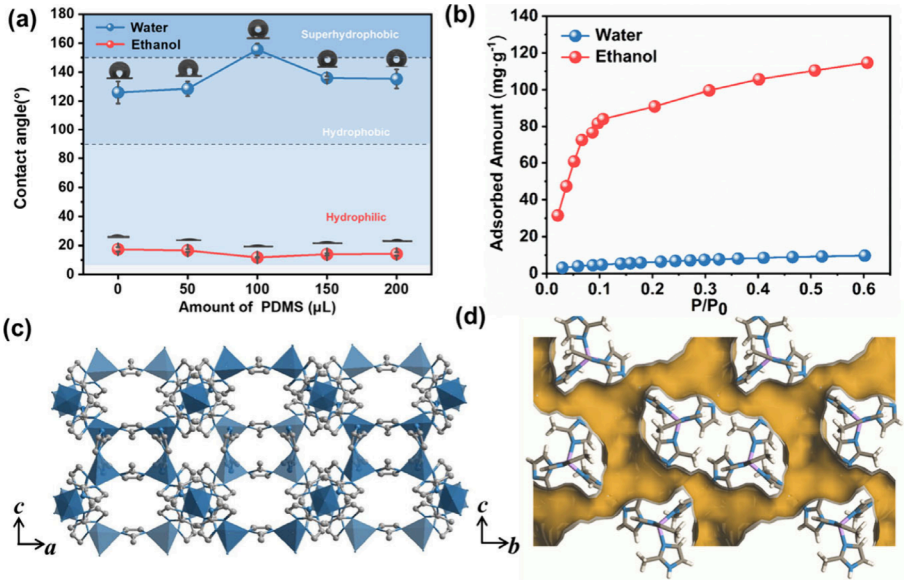

Figure 4. (a) Water and ethanol contact angles of ZIF-L membrane spin-coated with different amounts of PDMS. (b) Water and ethanol sorption isomers at 298 K of ZIF-L nanosheets. (c) Structure of ZIF-L nanosheet. (d) Interlayer channels of ZIF-L nanosheet.

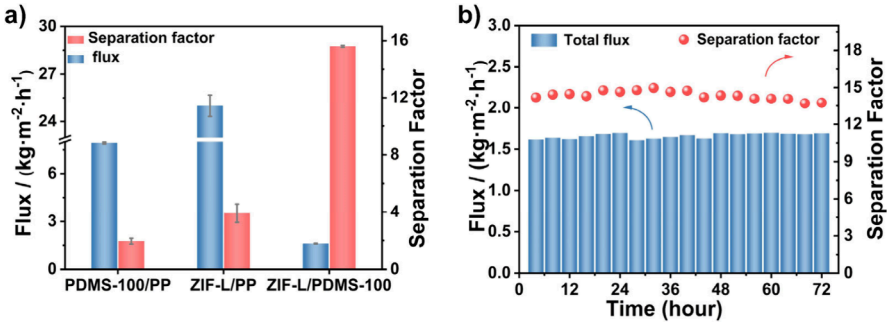

Figure 5. (a) Pervaporation performance for separating 5 wt % ethanol from aqueous solution at 60 °C. (b) Long-term test pervaporation performance of ZIF-L/PDMS-100 membrane for separating 5 wt % ethanol from aqueous solution at 60 °C.

capacities for ethanol and water are 115 $mg·g^{-1}$ and 9.6 $mg·g^{-1}$, respectively (Figure 4b). Ethanol molecules are absorbed preferentially over water molecules on ZIF-L nanosheets, and the appropriate exposure of ZIF-L nanosheets is beneficial for pervaporation separation. The N_2 adsorption−desorption isotherm calculated BET surface area of the ZIF-L nanosheet is 155 $m^2\ g^{-1}$ (Figure S9), aligning with the reported literature. Furthermore, structural analysis reveals that the pore diameters of ZIF-L (3.4 Å) nanosheets are oriented perpendicular to the two-dimensional crystal layers, which have interlayer pad-shaped cavities (9.4 Å × 7.0 Å × 5.3 Å) that are suitable for accommodating small molecules. Ethanol (4.3 Å) could readily diffuse through the ZIF-L pores, due to the "gate opening" effect of the flexible pore structure of ZIF-L. The channels aligned in the *b*-orientation are perpendicular to the movement of the guest molecules, resulting in a significant reduction in the transmission resistance of ethanol molecules. (Figure 4c, d). Therefore, the *b*-oriented ZIF-L/PDMS membrane with high surface roughness and superhydrophobic and ethanol affinity can enhance the selective adsorption separation of guest molecules on the membrane surface.

3.2. Pervaporation Separation Performance of the ZIF-L Membranes. Before the pervaporation test, the mixed gas separation performance of the ZIF-L/PDMS-100 membrane was initially tested to ensure no defects. The H_2 permeance is 127 GPU (4.27×10^{-8} $mol·m^{-2}·s^{-1}·Pa^{-1}$), and the separation factor is 5.58, which exceeding the corresponding Knudsen selectivity, indicating that the ZIF-L/PDMS-100 membrane is compact (Figure S10). Then the performance of the ZIF-L/PDMS composite membrane with superhydrophobic and strong ethanol affinity properties for separating ethanol from aqueous solution was investigated. As shown in Figure 5a, the flux of the PDMS-100/PP membrane was 7.92 $kg·m^{-2}·h^{-1}$, but the separation factor was only 1.96. The ZIF-L nanosheets grown on PP substrate significantly increase the flux to 25 $kg·m^{-2}·h^{-1}$, which is three times higher than that of the PDMS-100/PP membrane. The vertically aligned ZIF-L nanosheets are interconnected to offer transport channels that are in line with the flow direction of the guest molecules, consequently diminishing the resistance to guest molecule transport. Although there was a significant increase in flux, the improvement in selectivity was not significantly improved. To further optimize the separation performance of ZIF-L membrane, PDMS layer was spin-coated onto the ZIF-L membrane. The resulting ZIF-L/PDMS-100 composite membrane achieved a total flux as high as an average of 1.63 $kg·m^{-2}·h^{-1}$, and the separation factor significantly increased to 14.89 (Table S1). This is due to the *b*-oriented arrangement of the ZIF-L nanosheets combined with PDMS to form an excellent dense micronanostructure, superhydrophobic surface, and the channels aligned in the *b*-

https://doi.org/10.1021/cbe.5c00006
Chem Bio Eng. 2025, 2, 332−340

Table 1. Comparison of Different Membranes Reported with the ZIF-L/PDMS-100 Membrane for Ethanol Water Separation

Membrane	Feed content	Feed temperature (°C)	Flux ($kg·m^{-2}·h^{-1}$)	Separation Factor	Refs
MOF-NS/PDMS	5% CH_3CH_2OH	40	6.8	8.9	27
K-MWCNT/PDMS	6% CH_3CH_2OH	60	1.472	10.1	30
MAF-6/PEBA	5% CH_3CH_2OH	60	4.446	5.6	31
MA-Silicate-1/PDMS	5% CH_3CH_2OH	60	2.207	13.4	32
ZIF-8 PDMS	5% CH_3CH_2OH	60	1.229	9.9	33
MIL-53/PDMS	5% CH_3CH_2OH	70	5.467	11.1	34
APTES-ZIF-90/PDMS	5% CH_3CH_2OH	40	0.223	16.8	35
PDMS−PTFPMS	5% CH_3CH_2OH	60	1.149	11.3	36
PDMS-ZIF-8/Torlon	5% CH_3CH_2OH	60	0.847	8.9	37
ZIF-8/PDMS	5% CH_3CH_2OH	60	2.6	13.1	38
ZIF-L/PDMS	5% CH_3CH_2OH	60	1	16.2	39
ZIF-L/PDMS	5% CH_3CH_2OH	40	1.12	12.3	40
PDMS@ZIF-8	5% CH_3CH_2OH	60	5.4	9.6	41
ZIF-L/PDMS-100	5% CH_3CH_2OH	60	1.63	14.89	This Work

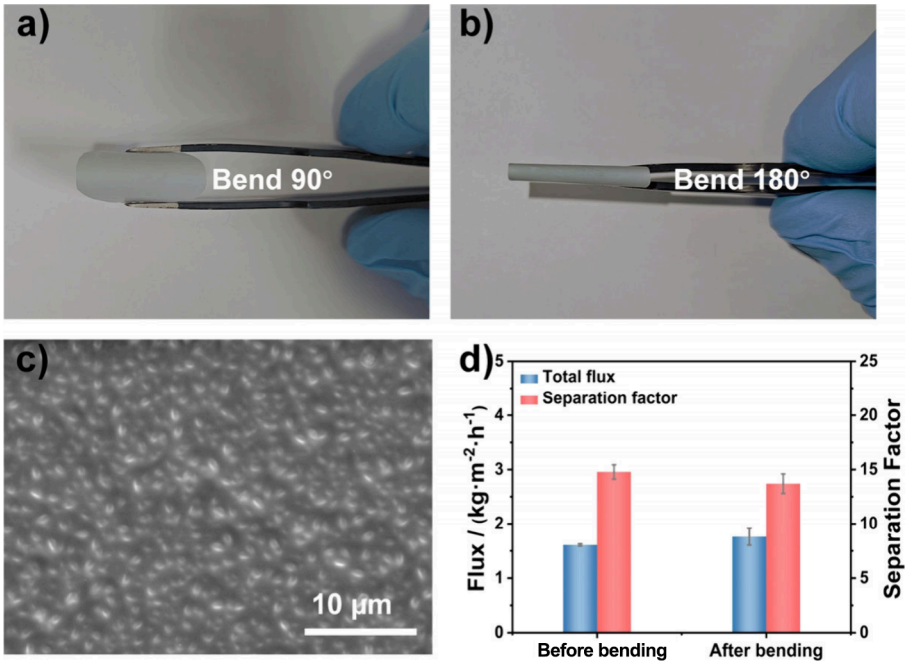

Figure 6. (a, b) Bending test of ZIF-L/PDMS-100 membrane with different curvature. (c) Top view SEM image of ZIF-L/PDMS-100 membrane after bending. (d) Pervaporation performance of ZIF-L/PDMS membrane before bending and after bending.

orientation of the ZIF-L nanosheets being more beneficial for the transport of ethanol molecules, thereby improving the separation performance. Figure S11 shows the effect of feed temperature on pervaporation performance at a feed concentration of 5 wt % ethanol aqueous. With the gradual increase in feed temperature, both the flux and separation factor also were improved. The increase of permeation flux and separation factor can be attributed to the enhanced flexibility of the PDMS polymer chains at higher temperatures, as well as the corresponding increase in the free volume of the cross-linked PDMS layer. Furthermore, as the temperature rises, the transmembrane vapor pressure difference between the various components also increases, thereby enhancing the driving force for the transport process. The apparent activation energy (E_A) can be calculated using the Arrhenius equation, which can analyze the effect of feed temperature on permeation behavior. The equation is as follows:

$$\ln Ji = \ln J_0 - \frac{E_{A,i}}{R \times T} \tag{3}$$

where J_0 denotes the Arrhenius constant for the permeation flux, R stands for the ideal gas constant, and T indicates the temperature of the feed in Kelvin (K). As shown in Figure S12, the calculated E_A value of ethanol (37.49 kJ/mol) is greater than that of water (23.03 kJ/mol). This substantial difference suggests that ethanol is more temperature sensitive, leading to preferential permeation of ethanol at higher temperatures. Thus, the separation factor improves as the feed temperature is elevated. In addition, to explore the practical application prospects of the material, the ZIF-L/PDMS-100 composite membrane underwent a long-term stability test. The ZIF-L/PDMS composite membrane can undergo a continuous 72 h permeation test, while the mass fraction of ethanol in feed side was increased from 5.0 to 45.2 wt % (Figure 5b). As a result, the ethanol concentration on the permeate side is five times that on the feed side.

https://doi.org/10.1021/cbe.5c00006
Chem Bio Eng. 2025, 2, 332−340

Benefiting from the combination of the oriented arrangement of ZIF-L nanosheets and the ultrathin PDMS layer, the ZIF-L/PDMS-100 composite membrane exhibits superhydrophobic and excellent ethanol-affinity surface. The exceptional surface properties of the membrane grant it high flux and good selectivity throughout the pervaporation process of separating ethanol from aqueous solution. This work showed excellent pervaporation performance of ethanol−water when compared to the previously reported membranes (Table 1).[27,30−41] Furthermore, polymer substrates typically exhibit good flexibility, making them easy to manipulate and apply in a variety of shapes and forms. After being subjected to bending at 180°, the surface of the ZIF-L/PDMS membrane remains intact without any cracks or defects; the vapor permeation shows nearly no changes after bending, indicating good flexibility of the ZIF-L/PDMS membrane (Figure 6). Therefore, this ZIF-L/PDMS membrane exhibits good potential for application in the field of separating ethanol from aqueous solution.

4. CONCLUSION

In summary, *b*-oriented ZIF-L membranes were rapidly synthesized on PP substrate by an electrochemical deposition method and then modified with an ultrathin PDMS layer, resulting in a superhydrophobic ZIF-L/PDMS composite membrane for efficiently separating ethanol from aqueous separation. In situ grown ZIF-L nanosheets exhibit vertically aligned nanochannels for guest molecules to pass through while the PDMS further enhances the hydrophobicity. The ZIF-L/PDMS membrane revealed a total flux of 1.63 $kg{\cdot}m^{-2}{\cdot}h^{-1}$ and separation factor of 14.89 during the pervaporation of 5 wt % ethanol aqueous solution. The mass fraction of ethanol in the feed side was increased from 5.0 to 45.2 wt.%, resulting in a 9 times increase in concentration. ZIF-L/PDMS composite membranes also exhibit good flexibility and long-term stability. This highly efficient membrane separation performance holds significant practical application value for the purification of biofuels in industrial production.

■ ASSOCIATED CONTENT

Supporting Information

The Supporting Information is available free of charge at https://pubs.acs.org/doi/10.1021/cbe.5c00006.

Rolling angle test video of ZIF-L/PDMS-100 membrane (MP4)

Pervaporation device schematic, structural characterization and surface analysis of ZIF-L and ZIF-L/PDMS membranes, gas and pervaporation testing results of ZIF-L/PDMS membrane (PDF)

■ AUTHOR INFORMATION

Corresponding Authors

Ming Xue − *School of Chemical Engineering and Technology, Sun Yat-sen University, Guangzhou 510275, P. R. China;* orcid.org/0000-0002-5011-3842; Email: xueming5@mail.sysu.edu.cn

Yi Li − *School of Chemical Engineering and Technology, Sun Yat-sen University, Guangzhou 510275, P. R. China;* Email: liyi266@mail.sysu.edu.cn

Authors

Wei Shao − *School of Chemical Engineering and Technology, Sun Yat-sen University, Guangzhou 510275, P. R. China*

Xiao-Feng Zhong − *School of Chemical Engineering and Technology, Sun Yat-sen University, Guangzhou 510275, P. R. China;* orcid.org/0000-0002-5639-2483

Yi-Le Chen − *School of Chemical Engineering and Technology, Sun Yat-sen University, Guangzhou 510275, P. R. China*

Zhen Chen − *School of Chemical Engineering and Technology, Sun Yat-sen University, Guangzhou 510275, P. R. China;* orcid.org/0000-0002-4566-6338

Miao-Miao Jia − *School of Chemical Engineering and Technology, Sun Yat-sen University, Guangzhou 510275, P. R. China*

Wen-Yong Yang − *School of Chemical Engineering and Technology, Sun Yat-sen University, Guangzhou 510275, P. R. China*

Jing-Ran Yu − *School of Chemical Engineering and Technology, Sun Yat-sen University, Guangzhou 510275, P. R. China*

Pan-Pan Zhang − *School of Chemical Engineering and Technology, Sun Yat-sen University, Guangzhou 510275, P. R. China*

Complete contact information is available at: https://pubs.acs.org/10.1021/cbe.5c00006

Author Contributions

Wei Shao: Methodology, Validation, Investigation, Writing-original draft, and Visualization. Xiao-Feng Zhong: Methodology. Yi-Le Chen: Methodology, Data curation. Zhen Chen, Miao−Miao Jia, Wen-Yong Yang, Jing-Ran Yu: Methodology. Pan-Pan Zhang: Methodology and Supervision. Yi Li: Methodology and Writing. Ming Xue: Conceptualization, Methodology, Writing-review and editing, Supervision, Project administration, and Funding acquisition.

Funding

This work was financially supported by National Natural Science Foundation of China (Nos. 22071076, 22090061, 22305270, 22408407), Department of Science and Technology of Guangdong Province (2024A1515010429), State Key Laboratory of Advanced Technology for Materials Synthesis and Processing (Wuhan University of Technology, 2023-KF-12), Postdoctoral Fellowship Program of CPSF (GZB20230882), and Science and technology planning project of Zhuhai (2320004000169) and Fundamental Research Funds for the Central Universities (24xkjc007), Sun Yat-sen University.

Notes

The authors declare no competing financial interest.

■ REFERENCES

(1) Mendiburu, A. Z.; Lauermann, C. H.; Hayashi, T. C.; Mariños, D. J.; Rodrigues da Costa, R. B.; Coronado, C. J. R.; Roberts, J. J.; de Carvalho, J. A., Jr Ethanol as a renewable biofuel: Combustion characteristics and application in engines. *Energy.* **2022**, *257*, 124688.

(2) Ragauskas, A. J.; Williams, C. K.; Davison, B. H.; Britovsek, G.; Cairney, J.; Eckert, C. A.; Frederick, W. J., Jr; Hallett, J. P.; Leak, D. J.; Liotta, C. L.; Mielenz, J. R.; Murphy, R.; Templer, R.; Tschaplinski, T. The path forward for biofuels and biomaterials. *Science.* **2006**, *311*, 484−489.

(3) Cai, D.; Wen, J.; Zhuang, Y.; Huang, T.; Si, Z.; Qin, P.; Chen, H. Review of alternative technologies for acetone-butanol-ethanol separation: Principles, state-of-the-art, and development trends. *Sep. Purif. Technol.* **2022**, *298*, 121244.

(4) Chen, X.; Li, N.; Wu, C.; Chen, L.; Zhou, Q. Enhancing Pervaporation Performance for Alcohol Recovery from Aqueous Solutions with Silicalite-1/Polydimethyldiethoxy silane (PDMDES) Nanocomposite Membranes. *Ind. Eng. Chem. Res.* **2024**, *63*, 508−524.

(5) Xia, W.; Yang, Y.; Sheng, L.; Zhou, Z.; Chen, L.; Zhang, Z.; Zhang, Z.; Yang, Q.; Ren, Q.; Bao, Z. Temperature-dependent molecular sieving of fluorinated propane/propylene mixtures by a flexible-robust metal-organic framework. *Sci. Adv.* **2024**, *10*, No. eadj6473.
(6) Luo, X.; Zhang, M.; Hu, Y.; Xu, Y.; Zhou, H.; Xu, Z.; Hao, Y.; Chen, S.; Chen, S.; Luo, W.; Lin, Y.; Zhao, J. Wrinkled metal-organic framework thin films with tunable Turing patterns for pliable intergration. *Science.* **2024**, *385*, 647−651.
(7) Li, L.; Guo, L.; Olson, D. H.; Xian, S.; Zhang, Z.; Yang, Q.; Wu, K.; Yang, Y.; Bao, Z.; Ren, Q.; Li, J. Discrimination of xylene isomers in a stacked coordination polymer. *Science* **2022**, *377*, 335−339.
(8) Imad, M.; Castro-Muñoz, R. Ongoing Progress on Pervaporation Membranes for Ethanol Separation. *Membranes.* **2023**, *13*, 848.
(9) Zhou, L.; Li, S.; Chen, Li; Li, Q.; Lu, C.; Tan, L.; Dong, L.; Zhou, C.; Cheng, J. MOFs and COFs based pervaporation membranes for alcohols/water separation: A review. *Sep. Purif. Technol.* **2024**, *330*, 125324.
(10) Chen, G.; Chen, C.; Guo, Y.; Chu, Z.; Pan, Y.; Liu, G.; Liu, G.; Han, Y.; Jin, W.; Xu, N. Solid-solvent processing of ultrathin, highly loaded mixed-matrix membrane for gas separation. *Science.* **2023**, *381*, 1350−1356.
(11) Howarth, A. J.; Liu, Y.; Li, P.; Li, Z.; Wang, T. C.; Hupp, J. T.; Farha, O. K. Chemical, Thermal and mechanical stabilities of metal-organic frameworks. *Nat. Rev. Mater.* **2016**, *1*, 15018.
(12) Yang, L.; Qian, S.; Wang, X.; Cui, X.; Chen, B.; Xing, H. Energy-efficient separation alternatives: metal-organic frameworks and membranes for hydrocarbon separation. *Chem. Soc. Rev.* **2020**, *49*, 5359−5406.
(13) Hou, Q.; Wu, Y.; Zhou, S.; Wei, Y.; Caro, J.; Wang, H. Ultra-Tuning of the Aperture Size in Stiffened ZIF-8_Cm Frameworks with Mixed-Linker Strategy for Enhanced CO_2/CH_4 Separation. *Angew. Chem., Int. Ed.* **2019**, *58*, 327−331.
(14) Li, X.; Liu, Y.; Wang, J.; Gascon, J.; Li, J.; der Bruggen, B. V. Metal-organic frameworks based membranes for liquid separation. *Chem. Soc. Rev.* **2017**, *46*, 7124−7144.
(15) Liu, X.; Li, Y.; Zhu, G.; Ban, Y.; Xu, L.; Yang, W. An Organophilic Pervaporation Membrane Derived from Metal-Organic Framework Nanoparticles for Efficient Recovery of Bio-Alcohols. *Angew. Chem., Int. Ed.* **2011**, *50*, 10636−10639.
(16) Gao, Z.; Li, B.; Ou, S.; Li, D.; Fang, Q.; Qiu, S.; Xue, M. Highly Durable MIL-96 Membranes via a One-step Active γ-Alumina Conversion Strategy for Gas Separation. *Chem. Res. Chinese U.* **2023**, *39*, 1084−1091.
(17) Song, Y.; Phipps, J.; Zhu, C.; Ma, S. Porous Materials for Water Purification. *Angew. Chem., Int. Ed.* **2023**, *62*, No. e202216724.
(18) Li, J.; Bhatt, P. M.; Li, J.; Eddaoudi, M.; Liu, Y. Recent Progress on Microfine Design of Metal−Organic Frameworks: Structure Regulation and Gas Sorption and Separation. *Adv. Mater.* **2020**, *32*, 2002563.
(19) Wei, R.; Liu, X.; Zhou, Z.; Chen, C.; Yuan, Y.; Li, Z.; Li, X.; Dong, X.; Lu, D.; Han, Y.; Lai, Z. Carbon nanotube supported oriented metal organic framework membrane for effective ethylene/ethane separation. *Sci. Adv.* **2022**, *8*, No. eabm6741.
(20) Li, H.; Han, L.; Hou, J.; Liu, J.; Zhang, Y. Oriented Zeolitic imidazolate framework membranes within polymeric matrices for effective N_2/CO_2 separation. *J. Membr. Sci.* **2019**, *572*, 82−91.
(21) Wang, S.; Liu, J.; Pulido, B.; Li, Y.; Mahalingam, D.; Nunes, S. P. Oriented Zeolitic Imidazolate Framework (ZIF) Nanocrystal Films for Molecular Separation Membranes. *ACS Appl. Nano Mater.* **2020**, *3*, 3839−3846.
(22) Zhang, C.; Yan, J.; Ji, T.; Du, D.; Sun, Y.; Liu, L.; Zhang, X.; Liu, Y. Fabrication of highly (110)-Oriented ZIF-8 membrane at low temperature using nanosheet seed layer. *J. Membr. Sci.* **2022**, *641*, 119915.
(23) Li, H.; Hou, J.; Bennett, T. D.; Liu, J.; Zhang, Y. Templated growth of vertically aligned 2D metal-organic framework nanosheets. *J. Mater. Chem. A* **2019**, *7*, 5811−5818.
(24) Zhong, Z.; Yao, J.; Chen, R.; Low, Z.; He, M.; Liu, J. Z.; Wang, H. Oriented two-dimensional zeolitic imidazolate framework-L membranes and their gas permeation properties. *J. Mater. Chem. A* **2015**, *3*, 15715−15722.
(25) Ma, X.; Wan, Z.; Li, Y.; He, X.; Caro, J.; Huang, A. Anisotropic Gas Separation in Oriented ZIF-95 Membranes Prepared by Vapor-Assisted In-Plane Epitaxial Growth. *Angew.Chem., Int. Ed.* **2020**, *59*, 20858−20862.
(26) Sun, Y.; Yan, J.; Gao, Y.; Ji, T.; Chen, S.; Wang, C.; Lu, P.; Li, Y.; Liu, Y. Fabrication of Highly Oriented Ultrathin Zirconium Metal-Organic Framework Membrane from Nanosheets towards Unprecedented Gas Separation. *Angew.Chem., Int. Ed.* **2023**, *62*, 20858−20862.
(27) Xu, L.-H.; Li, S.-H.; Mao, H.; Li, Y.; Zhang, A.-S.; Wang, S.; Liu, W.-M.; Lv, J.; Wang, T.; Cai, W.-W.; Sang, L.; Xie, W.-W.; Pei, C.; Li, Z.-Z.; Feng, Y.-N.; Zhao, Z.-P. Highly flexible and superhydrophobic MOF nanosheet membrane for ultrafast alcohol-water separation. *Science.* **2022**, *378*, 308−313.
(28) Shu, L.; Peng, Y.; Yao, R.; Song, H.; Zhu, C.; Yang, W. Flexible Soft-Solid Metal−Organic Framework Composite Membranes for H_2/CO_2 Separation. *Angew.Chem., Int. Ed.* **2022**, *61*, No. e202117577.
(29) Sun, H.; Wang, N.; Xu, Y.; Wang, F.; Lu, J.; Wang, H.; An, Q.-F. Aromatic-aliphatic hydrocarbon separation with oriented monolayer polyhedral membrane. *Science* **2024**, *386*, 1037−1042.
(30) Tian, Y.; Hu, C.; An, M.; He, X.; Wang, H.; Yi, C. Fabrication and Characterization of Carbon Nanotube Filled PDMS Hybrid Membranes for Enhanced Ethanol Recovery. *ACS Appl. Mater. Interfaces* **2023**, *15*, 12294−12304.
(31) Liu, Q.; Li, Y.; Li, Q.; Liu, G.; Liu, G.; Jin, W. Mixed-matrix hollow fiber composite membranes comprising of PEBA and MOF for pervaporation separation of ethanol/water mixtures. *Sep. Purif. Technol.* **2019**, *214*, 2−10.
(32) Si, Z.; Li, G.; Wang, Z.; Cai, D.; Li, S.; Baeyens, J.; Qin, P. A Particle-Driven, Ultrafast-Cured Strategy for Tuning the Network Cavity Size of Membranes with Outstanding Pervaporation Performance. *ACS Appl. Mater. Interfaces* **2020**, *12*, 31887−31895.
(33) Yan, H.; Li, J.; Fan, H.; Ji, S.; Zhang, G.; Zhang, Z. Sonication-enhanced in situ assembly of organic/inorganic hybrid membranes: Evolution of nanoparticle distribution and pervaporation performance. *J. Membr. Sci.* **2015**, *481*, 94−105.
(34) Zhang, G.; Li, J.; Wang, N.; Fan, H.; Zhang, R.; Zhang, G.; Ji, S. Enhanced flux of polydimethylsiloxane membrane for ethanol permselective pervaporation via incorporation of MIL-53 particles. *J. Membr. Sci.* **2015**, *492*, 322−330.
(35) Han, Z.; Zhao, Y.; Jiang, H.; Sheng, A.; Li, H.; Jia, H.; Yun, Z.; Wei, Z.; Wang, H. (3-Aminopropyl)Triethoxysilane-Modified ZIF-90 Nanoparticle/Polydimethylsiloxane Mixed Matrix Membranes for Ethanol Recovery via Pervaporation. *ACS Appl. Nano Mater.* **2022**, *5*, 183−194.
(36) Liu, C.; Xue, T.; Yang, Y.; Ouyang, J.; Chen, H.; Yang, S.; Li, G.; Cai, D.; Si, Z.; Li, S.; Qin, P. Effect of crosslinker 3-methacryloxypropylmethyldimethoxysilane on UV-crosslinked PDMS-PTFPMS block copolymer membranes for ethanol pervaporation. *Chem. Eng. Res. Des.* **2021**, *168*, 13−24.
(37) Li, J.; Labreche, Y.; Wang, N.; Ji, S.; An, Q. PDMS/ZIF-8 coating polymeric hollow fiber substrate for alcohol permselective pervaporation membranes. *Chinese. J. Chem. Eng.* **2019**, *27*, 2376−2382.
(38) Cai, P.; Zhang, N.; Wang, Y.; Li, J.; Wang, N.; Meng, H.; An, Q. In-situ growth of ZIF-8/PDMS membrane at the liquid−liquid interface for efficient ethanol recovery. *Sep. Purif. Technol.* **2025**, *362*, 131872.
(39) Mao, H.; Zhen, H.; Ahmad, A.; Li, S.; Liang, Y.; Ding, J.; Wu, Y.; Li, L.; Zhao, Z. Highly selective and robust PDMS mixed matrix membranes by embedding two-dimensional ZIF-L for alcohol permselective pervaporation. *J. Membr. Sci.* **2019**, *582*, 307−321.
(40) Pei, C.; Mao, H.; Wang, Y. J.; Liu, W.; Li, Z.; Xie, W.; Li, Y.; Zhao, Z. Boosting pervaporation performance of ZIF-L/PDMS mixed matrix membranes by surface plasma etching for ethanol/water separation. *Sep. Purif. Technol.* **2023**, *318*, 124025.
(41) Liu, W.; Chen, X.; Mao, H.; Li, S.; Zhang, Y.; Xu, L.; Zhao, Z. Construction of PDMS@ZIF-8 composite membrane on PVDF hollow

https://doi.org/10.1021/cbe.5c00006
Chem Bio Eng. 2025, 2, 332−340

fiber inner surface for ultrafast ethanol/water separation. *J. Membr. Sci.* **2024**, *704*, 122889.

https://doi.org/10.1021/cbe.5c00006
Chem Bio Eng. 2025, 2, 332−340